Plant Cell Physiol. 48(3): 391–404 (2007)
doi:10.1093/pcp/pcm008, available online at www.pcp.oxfordjournals.org
© The Author 2007. Published by Oxford University Press on behalf of Japanese Society of Plant Physiologists.
All rights reserved. For permissions, please email: journals.permissions@oxfordjournals.org

Overexpression of miR165 Affects Apical Meristem Formation, Organ Polarity Establishment and Vascular Development in *Arabidopsis*

Gong-Ke Zhou [1], Minoru Kubo [2], Ruiqin Zhong [1], Taku Demura [2] and Zheng-Hua Ye [1,*]

[1] *Department of Plant Biology, University of Georgia, Athens, GA 30602, USA*
[2] *RIKEN Plant Science Center, Yokohama, Kanagawa, 230-0045 Japan*

The class III homeodomain leucine-zipper (*HD-ZIP III*) genes are thought to be targets of microRNAs (miRNAs) 165 and 166, but it is not known whether all the developmental processes affected by mutations of the *HD-ZIP III* genes could be recapitulated by an alteration in the expression of miR165 and miR166. Previous work showed that overexpression of miR166 by activation tagging results in down-regulation of the *ATHB-9*|*PHV*, *ATHB-14*|*PHB* and *ATHB-15* genes, and concomitantly causes an enlargement of shoot apical meristems (SAMs) and an enhancement in vascular development. Here we demonstrated that overexpression of miR165 causes a drastic reduction in the transcript levels of all five *HD-ZIP III* genes in *Arabidopsis*. The miR165 overexpressors display prominent phenotypes reminiscent of loss-of-function mutants of *rev phb phv* and *rev*|*ifl1*, including loss of SAM, alteration of organ polarity, abnormal formation of carpels, inhibition of vascular development and aberrant differentiation of interfascicular fibers. Global gene expression analysis revealed a link between miR165 overexpression and altered expression of genes involved in auxin signaling and vascular development. Our results demonstrate that overexpression of miR165 recapitulates the phenotypes caused by loss-of-function mutations of *HD-ZIP III* genes, such as loss of SAM, altered organ polarity and defects in development of vascular tissues and interfascicular fibers.

Keywords: *Arabidopsis thaliana* — Homeodomain proteins — Meristem — MicroRNA — Organ polarity — Vascular development.

Abbreviations: CaMV, cauliflower mosaic virus; DIG, digoxigenin; HD-ZIP, homeodomain leucine-zipper protein; RT–PCR, reverse transcription–PCR; SAM, shoot apical meristem.

Introduction

MicroRNAs (miRNAs) are ~21 nucleotide non-coding RNAs that regulate the expression of target genes by binding to the complementary sequences located in their transcripts. Such binding of miRNAs to their target sequences can lead to translational attenuation or target the mRNAs for cleavage and degradation (Kinder and Martiensen 2005a). In plants, several hundred miRNAs have been identified from a diverse group of species and, of them, many putative target genes have been predicted (Dugas and Bartel 2004, Kidner and Martienssen 2005a, Zhang *et al*. 2006). It has been shown that miRNAs are first transcribed by RNA polymerase II to produce pri-miRNAs, which are then processed by DICER-like proteins and other components into mature miRNAs (Kurihara and Watanabe 2004). Mutations of genes involved in miRNA processing have been shown to cause pleiotropic effects (Dugas and Bartel 2004, Kidner and Martienssen 2005a). Mature miRNAs are incorporated into the RISC complex, which is responsible for cleavage of the target mRNAs or inhibition of their translation (Kidner and Martienssen 2005a). The functions of a number of miRNAs in plants have been demonstrated by overexpression or knockout studies and by characterization of their target genes. These studies revealed important roles for miRNAs in diverse processes of plant growth and development (Dugas and Bartel 2004, Chen 2005, Jover-Gil *et al*. 2005, Kidner and Martienssen 2005a, Zhang *et al*. 2006).

One of the best characterized miRNAs in plants is miR165/166. Mature miR165/166 are predicted to have 21 nucleotides, and their sequences differ by only one nucleotide. Two copies of miR165 and six of miR166 are present in the *Arabidopsis* genome (Reinhart *et al*. 2002). miR165/166 have been shown to be localized in the shoot apical meristem (SAM), leaf primordia and vascular tissues in *Arabidopsis* (Kidner and Martienssen 2004, Li *et al*. 2005, Williams *et al*. 2005). Based on sequence analysis, the *HD-ZIP III* genes, namely *IFL1*|*REV*, *ATHB-9*|*PHV*, *ATHB-14*|*PHB*, *ATHB-8* and *ATHB-15*|*CNA*|*ICU4*, are predicted to be target genes for miR165/166. The mRNAs of *ATHB-14*|*PHB* and *ATHB-15* have been shown to be cleaved at the miR165/166 target sequence in biochemical assays (Tang *et al*. 2003, Kim *et al*. 2005). The important roles of miR165/166 in the regulation of *HD-ZIP III* genes were revealed by studies of dominant mutations of the *HD-ZIP III* genes. Mutations of the miR165/166 target sequences of *HD-ZIP III* lead to resistance to cleavage and consequently cause dominant phenotypes, including

*Corresponding author: E-mail, zhye@plantbio.uga.edu; Fax,+1-706-542-1805.

Downloaded from https://academic.oup.com/pcp/article/48/3/391/2329589 by guest on 21 August 2022

alterations in meristem functions, organ polarity, and vascular differentiation and patterning (McConnell *et al*. 2001, Emery *et al*. 2003, Juarez *et al*. 2004, McHale and Koning 2004, Zhong and Ye 2004, Kim *et al*. 2005, Ohashi-Ito *et al*. 2005, Ochando *et al*. 2006). These analyses clearly indicate that tight regulation of the *HD-ZIP III* transcript levels by miR165/166 is essential for their normal functions.

Loss-of-function mutations of the *HD-ZIP III* genes have been demonstrated to affect various aspects of plant growth and development. It has been shown that loss-of-function mutations of *IFL1*/*REV* cause defects in lateral meristem formation, interfascicular fiber differentiation, secondary xylem development and polar auxin transport (Zhong and Ye 1999, Otsuga *et al*. 2001, Zhong and Ye 2001). Although loss-of-function mutations of individual *ATHB-9*/*PHV*, *ATHB-14*/*PHB* or *ATHB-8* genes do not show any phenotypes, simultaneous loss-of-function mutations of *IFL1*/*REV*, *ATHB-9*/*PHV* and *ATHB-14*/*PHB* cause a loss of SAM and formation of pin-like cotyledons (Prigge *et al*. 2005). However, it is not clear whether all these developmental processes could be affected by an alteration in miR165/166 expression.

Because miRNAs are thought to regulate the mRNA level of their target genes in plants, overexpression of miRNAs is predicted to cause a severe down-regulation of their target mRNAs and thereby should recapitulate the loss-of-function phenotypes of their target genes. Overexpression of miR166a or miR166g by activation tagging has been shown to result in a reduction in the mRNA levels of *ATHB-9*/*PHV*, *ATHB-14*/*PHB* and *ATHB-15*, and a concomitant enlargement of SAMs and an alteration in vascular development (Kim *et al*. 2005, Williams *et al*. 2005). Although these phenotypes are reminiscent of the *phv phb cna* triple mutant (Prigge *et al*. 2005), they clearly do not phenocopy the defects exhibited by loss-of-function mutations of *IFL1*/*REV* or simultaneous loss-of-function mutations of *IFL1*/*REV*, *ATHB-9*/*PHV* and *ATHB-14*/*PHB*. This could be due to differential roles of miR165 and miR166 in the regulation of *HD-ZIP III* genes.

In this report, we studied the effects of miR165 overexpression on plant growth and development. We demonstrate that miR165 overexpression causes a drastic reduction in the transcript levels of all five *HD-ZIP III* genes and concomitantly recapitulates their loss-of-function mutation phenotypes, including loss of SAM, altered organ polarity, defective vascular development and impaired interfascicular fiber differentiation. These results suggest that miR165 plays an important role in regulation of such processes as normal SAM formation, organ polarity maintenance and vascular development. We further show that miR165 overexpression leads to an alteration in the expression of a number of genes involved in auxin signaling and vascular development.

Results

Overexpression of miR165 impairs shoot apical meristem formation

To investigate the roles of miR165 in plant development, we generated transgenic *Arabidopsis* plants showing overexpression of miR165. The *Arabidopsis* genome contains two miR165 genes, miR165a and miR165b, which are located on chromosome 1 and 4, respectively (Reinhart *et al*. 2002). Since the mature forms of miR165a and miR165b are identical, we have chosen one of them, miR165a, for overexpression under the cauliflower mosaic virus (CaMV) 35S promoter. The two neighboring genes At1g01180 and At1g01190, are about 1.5 and 4 kb, respectively, away from the predicted mature miR165a sequence. Three constructs with different lengths of the miR165a genomic sequence (Fig. 1A) were used for overexpression, and all of them exhibited the same effects on plant development. Thus the results from transgenic plants with overexpression of miR165a-1 in comparison with the control transgenic plants transformed with the vector alone are presented throughout this report. Striking phenotypes were evident in the seedlings of the first generation of transgenic plants (Fig. 1C, D). About 37% of transgenic seedlings did not develop a SAM. Among these, some seedlings had only one cotyledon and, in some cases, they were extremely radialized forming a pin-like structure. Others had two narrow cotyledons with either a pin structure or one terminal leaf in place of a SAM. Although the rest of the transgenic seedlings had a SAM, some of them displayed narrow cotyledons and small leaves. Longitudinal sections confirmed that whereas the wild-type seedlings had a dome-shaped SAM surrounded by many leaf primordia, a significant number of miR165 overexpressors did not develop such a dome-shaped apical meristem. These results demonstrate that overexpression of miR165 causes a severe effect on SAM formation.

Another prominent phenotype of the miR165 overpressors was the appearance of red pigments in the narrow cotyledons (Fig. 1D), which was most probably due to an accumulation of anthocyanin. The red pigments were not evident in the small leaves of miR165 overexpressors (Fig. 1C) and were not observed in the cotyledons of control transgenic plants under the same growth conditions (Fig. 1B).

To know whether the abnormal phenotypes of the transgenic seedlings correlated with an increased accumulation of miR165 transcript, we used both reverse transcription–PCR (RT–PCR) and RNA gel blot hybridization to detect miR165 RNA. miRNAs are known to be transcribed

Downloaded from https://academic.oup.com/pcp/article/48/3/391/2329589 by guest on 21 August 2022

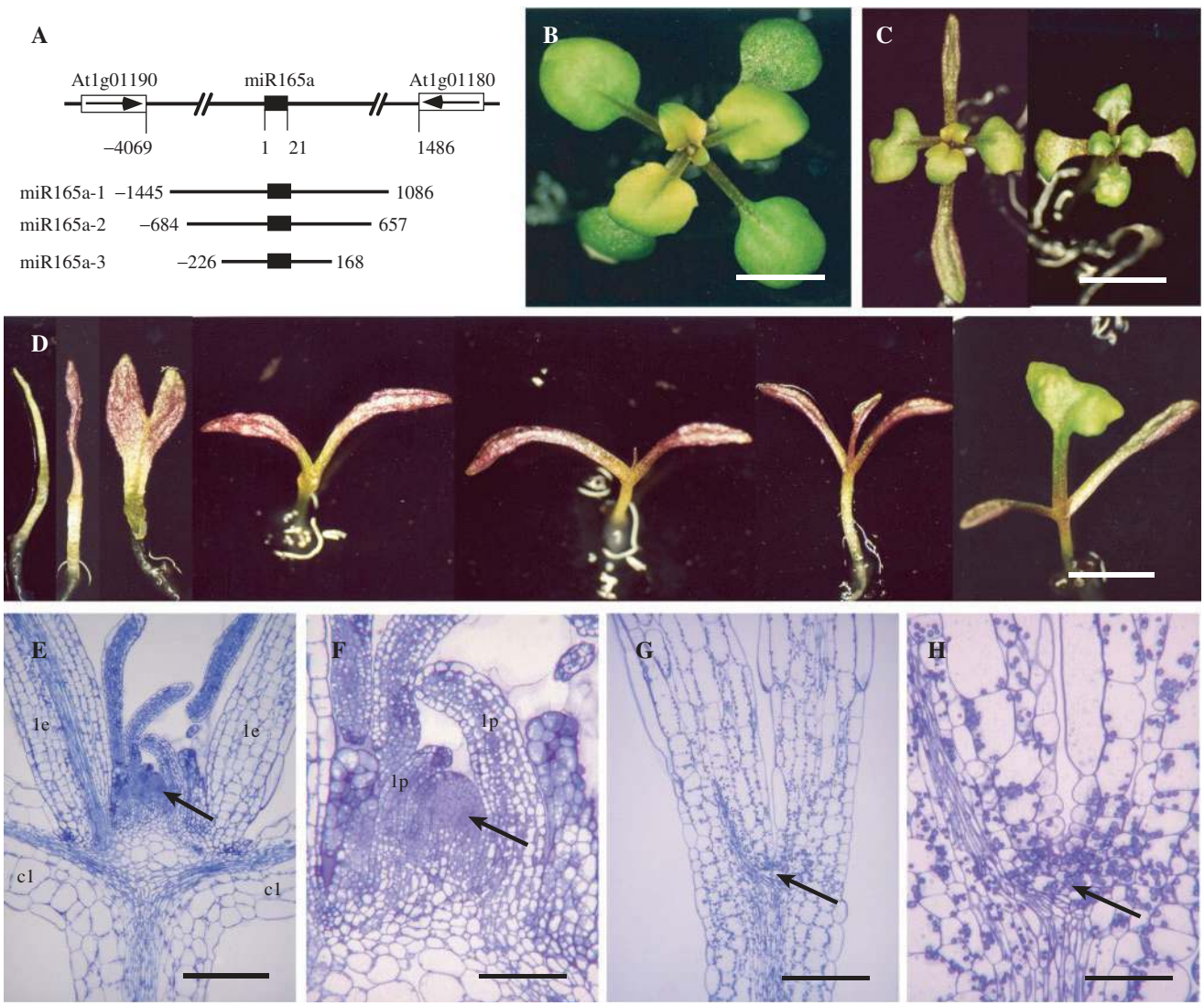

Fig. 1 Effects of miR165 overexpression on seedling development. (A) Diagram of the miR165a gene and its neighboring genes. Three DNA fragments containing the miR165a gene (miR165a-1, miR165a-2 and miR165a-3) were used for overexpression. (B) Twelve-day-old control transgenic seedling transformed with the vector alone. (C) Twelve-day-old miR165 overexpressors with narrow or small cotyledons and small leaves. (D) Twelve-day-old miR165 overexpressors having pin-like cotyledons, or two narrow cotyledons with a terminal pin or a leaf-like structure. (E) Medial longitudinal section of a control seedling showing SAM (arrow), cotyledons and leaves. (F) High magnification of (E) showing SAM (arrow) and its surrounding leaf primordia. (G) Medial longitudinal section of a miR165 overexpressor with two narrow cotyledons. (H) High magnification of (G) showing the absence of a dome-shaped SAM (arrow). cl, cotyledon; le, leaf; lp, leaf primordium. Scale bars = 5.2 mm in (B), 3.6 mm in (C), 2.2 mm in (D), 220 μm in (E) and (G), and 72 μm in (F) and (H).

as precursor forms and then processed into mature forms with 20–24 nucleotides (Kidner and Martienssen 2005a). We first applied RT–PCR to detect miR165a precursors. It was found that both the transgenic seedlings without SAM and those with small leaves accumulated a higher level of miR165a precursor RNA compared with the control (Fig. 2A). RNA gel blot analysis revealed that although mature miR165 RNA was not detectable in the control seedlings under the conditions used, it was evident in miR165 overexpressors with small leaves and accumulated at a very high level in those without a SAM (Fig. 2B). These results demonstrate that the abnormal seedling development in the miR165 overexpressors is correlated with an increased level of miR165 RNA.

Overexpression of miR165 down-regulates the expression of HD-ZIP III target genes and inhibits vascular development

The five *HD-ZIP III* genes, *IFL1*/*REV*, *ATHB-9*/*PHV*, *ATHB-14*/*PHB*, *ATHB-8* and *ATHB-15*, are considered to be targets of miR165/miR166 (Rhoades *et al*. 2002).

Downloaded from https://academic.oup.com/pcp/article/48/3/391/2329589 by guest on 21 August 2022

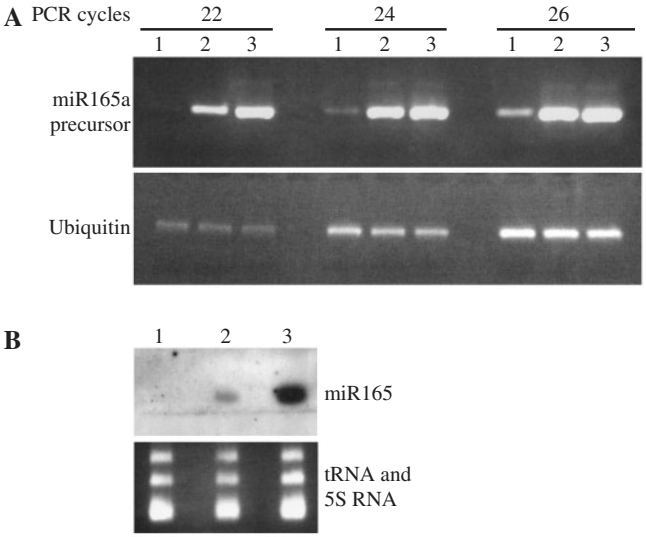

Fig. 2 Accumulation of miR165a precursor and mature miR165 in miR165 overexpressors. (A) Semi-quantitative RT–PCR analysis of the miR165a precursor. Total RNA was from the seedlings of control (1), miR165 overexpressors with small cotyledons and leaves (2) and with no SAM (3). Primers located at 225 nucleotides upstream and 145 nucleotides downstream of the mature miR165a sequence were used to PCR-amplify the miR165a precursor for various cycles. The expression of a ubiquitin gene was used as an internal control. (B) RNA gel blot analysis of the accumulation of mature miR165 in seedlings of the control (1) and miR165 overexpressors (2 and 3). miR165 was detected by hybridization with a digoxigenin-labeled antisense miR165 probe and subsequent detection with the chemiluminiscent method. Equal loading of RNA in each lane was confirmed by visualization of tRNAs and 5S RNA.

miR165 has 18 nucleotides completely matched with the target sequences in *HD-ZIP III* genes, except for *ATHB-15* with one additional mismatch (Fig. 3A), whereas miR166 has 18 nucleotides matched with the target sequence in *ATHB-15*. RT–PCR and quantitative real-time PCR analyses showed that overexpression of miR165 caused a drastic reduction in the expression levels of all *HD-ZIP III* genes (Fig. 3B, C). The mRNA levels of *HD-ZIP III* genes were reduced 5- to 8-fold in the miR165 overexpressors compared with those of the control plants.

Because *HD-ZIP III* genes have been shown to be important for vascular development (McConnell and Barton 1998, Zhong *et al*. 1999, Ohashi-Ito *et al*. 2002, Ohashi-Ito and Fukuda 2003, Green *et al*. 2005, Kim *et al*. 2005, Ohashi-Ito *et al*. 2005), we examined the venation patterns in the miR165 overexpressors. Although the cotyledons of control seedlings displayed a prominent midvein connected to lateral veins (Fig. 4A), the vein development in the miR165 overexpressors was severely impaired (Fig. 4B, C). Veins were generally absent in the cotyledons of seedlings without a SAM. Cross-sections of cotyledons confirmed that whereas the vascular bundles

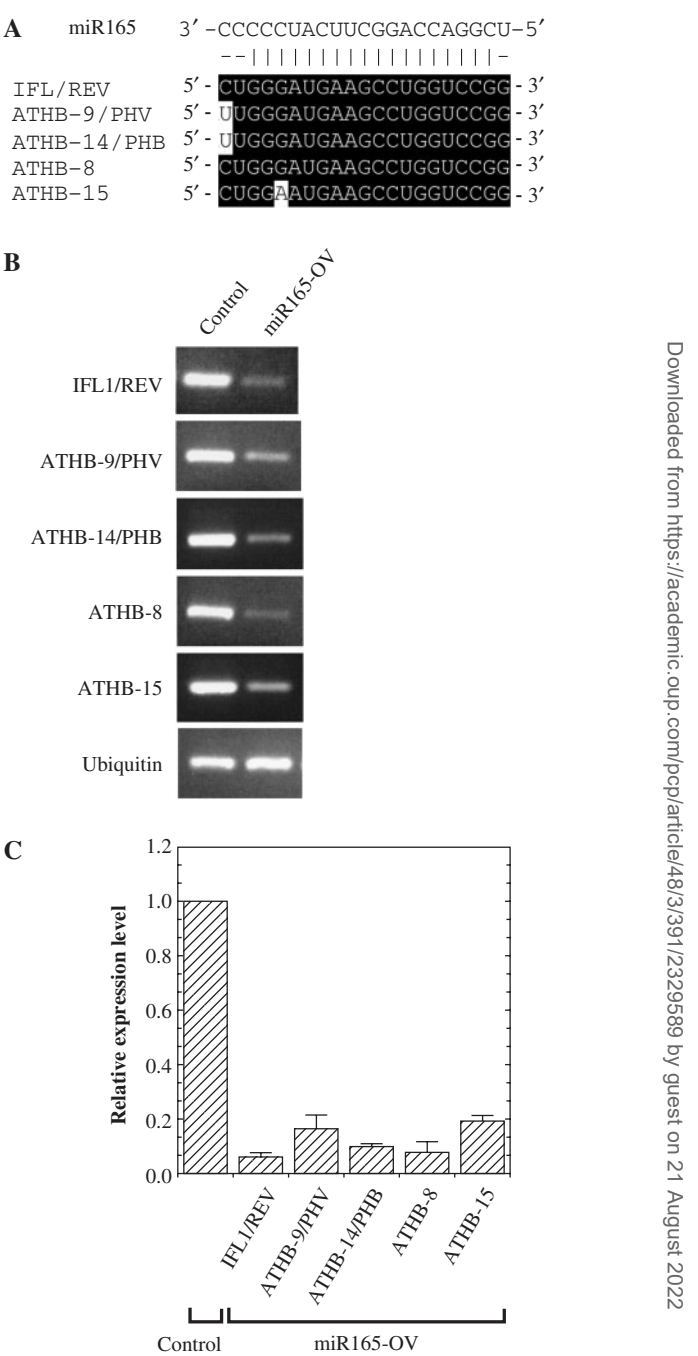

Fig. 3 Down-regulation of expression of *HD-ZIP III* genes by miR165 overexpression. (A) miR165 and its complementary target sequences in *Arabidopsis HD-ZIP III* mRNAs. (B) RT–PCR analysis of the expression levels of *HD-ZIP III* genes in the control and miR165 overexpressors (miR165-OV). The primers used were located on either side of the miR165 target sequences so that only the full-length *HD-ZIP III* mRNAs could be used as templates. The expression of a ubiquitin gene was used as an internal control. (C) Quantitative real-time PCR analysis of the expression levels of *HD-ZIP III* genes in the control and miR165 overexpressors. The expression level of each gene in the control is set to 1. The error bars represent the standard error of triplicate samples.

Downloaded from https://academic.oup.com/pcp/article/48/3/391/2329589 by guest on 21 August 2022

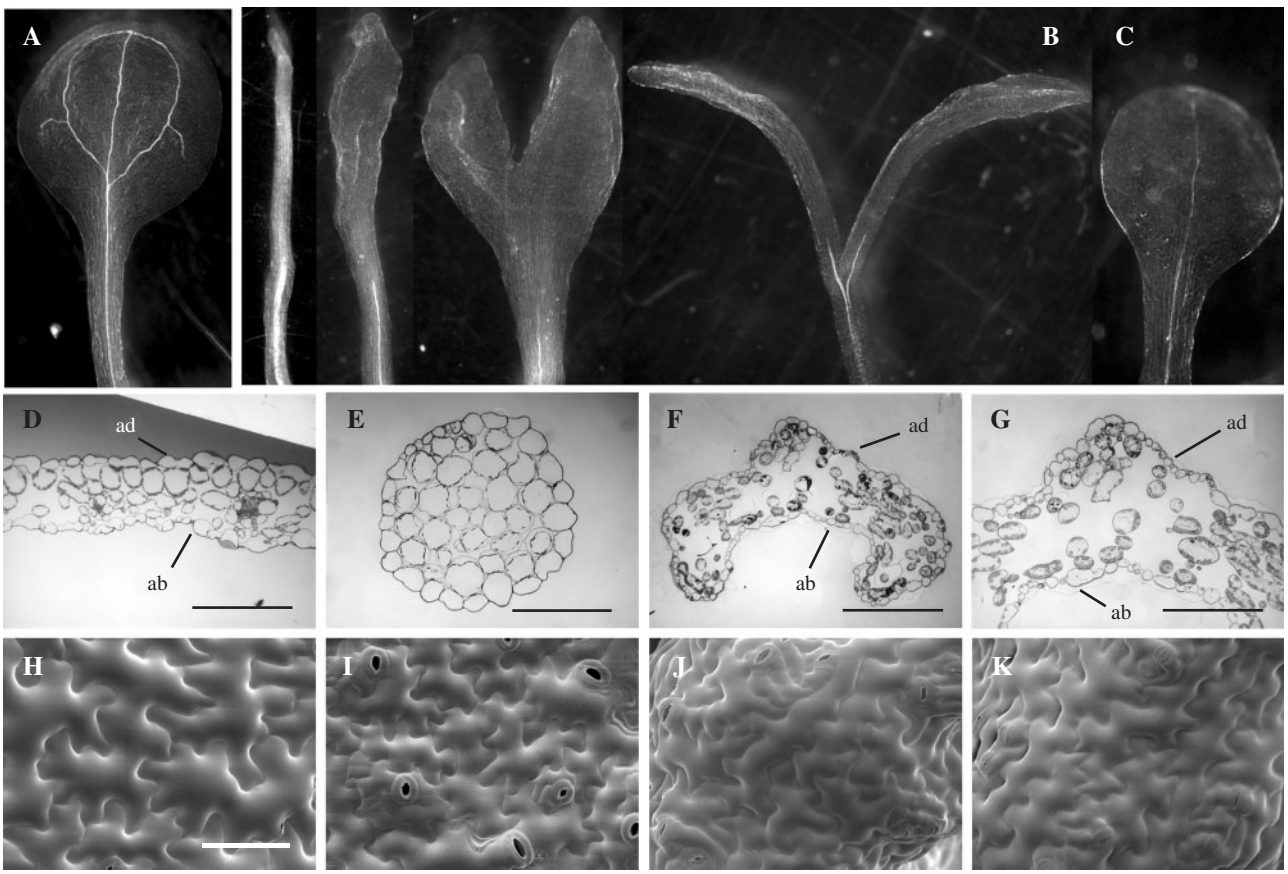

Fig. 4 miR165 overexpression inhibits vascular development and alters the polarity of cotyledons. (A) Cleared control cotyledon showing the midvein and looped secondary veins. (B) Cleared cotyledons of miR165 overexpressors with no SAM showing the absence of veins. Note the presence of vascular strands in hypocotyls. (C) Small cotyledon of miR165 overexpressors showing the presence of a midvein but the absence of secondary veins. (D) Cross-section of a control cotyledon showing the distinct arrangement of large and closely packed palisade cells on the adaxial side, and small and loosely packed spongy mesophyll cells on the abaxial side. (E) Cross-section of a pin-like cotyledon from miR165 overexpressors showing symmetrically arranged cells. (F) Cross-section of a narrow cotyledon from miR165 overexpressors showing lack of the distinct arrangement of mesophyll cells. (G) High magnification of (F) showing loosely packed mesophyll cells. (H) The adaxial surface of a control cotyledon showing large ordinary epidermal cells. (I) The abaxial surface of a control cotyledon showing smaller ordinary epidermal cells and the presence of many stomata. (J) and (K) Adaxial (J) and abaxial (K) surfaces of a narrow cotyledon from miR165 overexpressors showing similar morphology for ordinary epidermal cells and the presence of stomata. Scale bars = 210 μm in (D) and (F), 167 μm in (E), 137 μm in (G) and 62 μm in (H)–(K).

were clearly visible in the control (Fig. 4D), they were absent in the cotyledons of miR165 overexpressors (Fig. 4E–G). In those with a SAM, the small cotyledons often had a midvein but lacked lateral veins (Fig. 4C). Although the leaves of these plants exhibited a normal venation pattern, the minor veins were not well developed compared with the control plants (Fig. 5K, L).

Overexpression of miR165 causes an alteration in organ polarity

The pin-shaped cotyledon phenotype seen in the miR165 overexpressors indicates an alteration in organ polarity. Examination of the organization and morphology of cells in the cotyledons revealed that although the cotyledons in the control seedlings had one layer of columnar-shaped palisade parenchyma cells at the adaxial (upper) side and loosely organized spongy mesophyll cells at the abaxial (lower) side (Fig. 4D), this organization was altered in the cotyledons of miR165 overexpressors. The pin-shaped cotyledons had round-shaped mesophyll cells packed closely together in a radially symmetrical manner (Fig. 4E). The mesophyll cells in the narrow cotyledons did not form a distinct layer of palisade cells, and instead they were loosely packed (Fig. 4F, G), resembling the organization of spongy mesophyll cells in wild-type cotyledons. Scanning electron microscopy of the cotyledon epidermis revealed that although the adaxial epidermis of control cotyledons had larger ordinary epidermal cells than the abaxial epidermis and no stomata (Fig. 4H, I), both the adaxial and abaxial epidermis of cotyledons of miR165

Downloaded from https://academic.oup.com/pcp/article/48/3/391/2329589 by guest on 21 August 2022

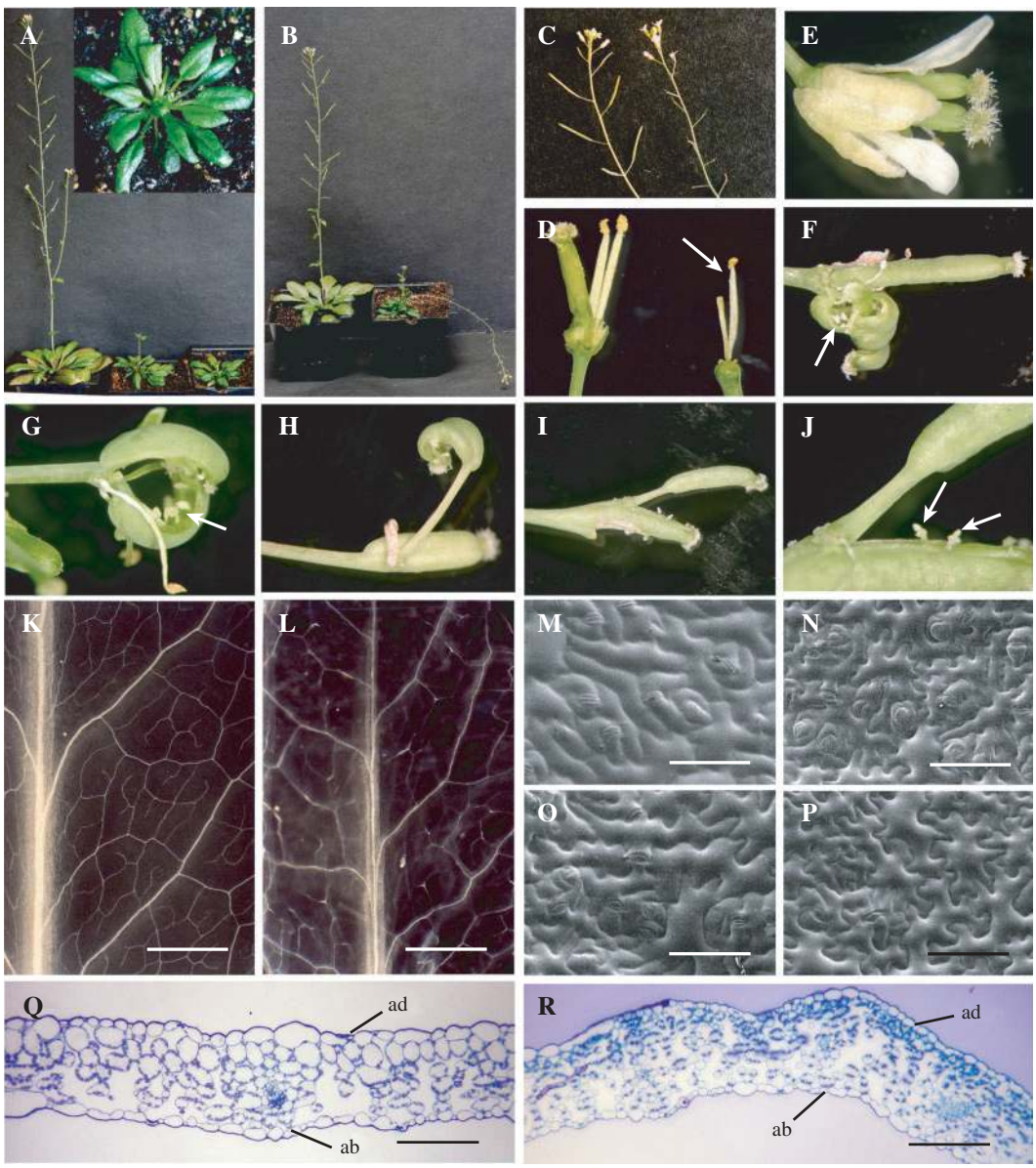

Fig. 5 Effects of miR165 overexpression on plant growth and development. (A) miR165 overexpression causes a reduction in rosette size (middle and right) compared with the control (left). The inset shows a high magnification of a miR165 overexpressor with dark-green and downward curling leaves. (B) Development of pendent inflorescence stems in miR165 overexpressors (right) compared with the control (left). (C) The inflorescence of miR165 overexpressors does not produce siliques (right) compared with the control (left). (D) Formation of filamentous carpel (arrow) in miR165 overexpressors (right) compared with the control (left). Sepals, petals and some stamens were removed for observation. (E)–(J) miR165 overexpression induces formation of aberrant carpels, including flowers with two carpels (E), multiple aberrant carpels with exposed ovules (arrow) (F and G), ectopic formation of carpels on top of another carpel (H and I) and production of aberrant structures (arrows) on the outer surface of siliques (J). (K) and (L) Cleared leaves showing reduced development of minor veins in miR165 overexpressors (L) compared with the control (K). (M) and (N) Scanning electron micrographs of control leaf epidermis showing that the anticlinal walls of ordinary epidermis on the adaxial surface (M) are much less sinuous than those on the abaxial surface (N). (O) and (P) Scanning electron micrographs of leaf epidermis of miR165 overexpressors showing that the anticlinal walls of ordinary epidermis on the adaxial surface (O) are nearly as sinuous as those on the abaxial surface (P). (Q) Cross-section of a control leaf showing large and closely packed palisade cells on the adaxial side and small and loosely packed spongy mesophyll cells on the abaxial side. (R) Cross-section of a leaf of miR165 overexpressors showing small and loosely packed mesophyll cells on both the adaxial and abaxial sides. Bars = 1 mm in (K) and (L), 75 μm in (M)–(P) and 135 μm in (Q) and (R).

Downloaded from https://academic.oup.com/pcp/article/48/3/391/2329589 by guest on 21 August 2022

overexpressors had stomata and small ordinary epidermal cells (Fig. 4J, K), resembling the wild-type abaxial epidermal identity.

Similarly, the columnar-shaped palisade cells as seen in the control leaves were not evident in the leaves of miR165 overexpressors, and instead the mesophyll cells appeared small and loosely packed (Fig. 5Q, R), resembling the abaxial identity. In addition, whereas the adaxial epidermal cells were much less sinuous than the abaxial ones in the control leaves (Fig. 5M, N), the epidermal cells on both sides of leaves of miR165 overexpressors were highly sinuous (Fig. 5O, P). These results demonstrate that miR165 overexpression causes development of abaxial characters in place of adaxial characters in both cotyledons and leaves.

Effects of miR165 overexpression on overall plant development

The transgenic seedlings without a SAM did not survive after they were transferred to soil. The seedlings with small cotyledons and leaves were able to survive and grow into adult plants. The rosette leaves of miR165 overexpressors were dark green with an uneven adaxial surface, and were much smaller compared with the control (Fig. 5A). The inflorescence stems of miR165 overexpressors were often pendent and easily broken by bending (Fig. 5B). Two prominent floral phenotypes were observed in the miR165 overexpressors. One group of plants had infertile flowers, and a close examination revealed that the carpel development was retarded (Fig. 5C, D), a phenotype also reported for miR166 overexpressors (Williams *et al*. 2005). Another group developed flowers with various defects in carpel development. While some flowers had two normal-looking carpels (Fig. 5E), others developed several abnormal carpels that were often unenclosed, thus exposing the ovules (Fig. 5F, G). In addition, it was also observed that sometimes a carpel or carpel-like structures grew on top of another carpel (Fig. 5H, J). Aberrant outgrowth of carpels was also seen in the *avb1* mutant with a mutation in the miR165 target sequence of *IFL1*/*REV* (Zhong and Ye, 2004). This suggests that proper regulation of the *HD-ZIP III* target genes by miR165 is important for the normal development of carpels.

Alteration of interfascicular fiber and vascular development in the inflorescence stems of miR165 overexpressors

The fact that the inflorescence stems of miR165 overexpressors were often pendent and easily broken suggests that the development of mechanical tissues, xylem and interfascicular fibers might be affected. Cross-sections of stems showed that the xylem bundles of miR165 overexpressors were much smaller compared with the control (Fig. 6A, B). This indicates that miR165 overexpression

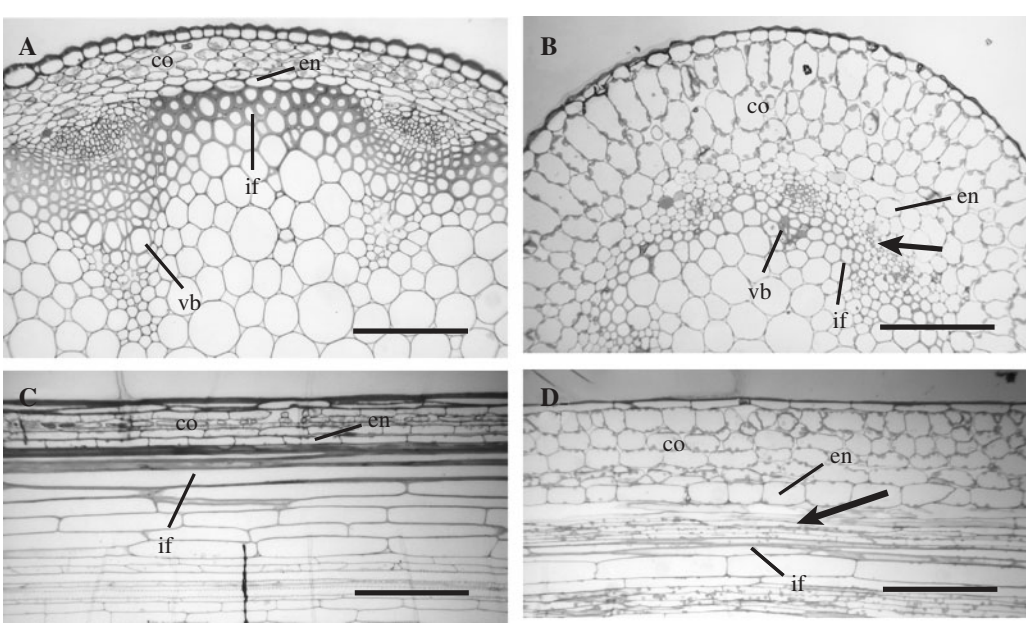

Fig. 6 Effects of miR165 overexpression on the development of vascular tissues and interfascicular fibers in stems. The basal parts of inflorescence stems from 10-week-old plants were used for examination. (A) Cross-section of a control stem showing vascular bundles and interfascicular fibers located next to the endodermis. (B) Cross-section of a stem of miR165 overexpressors showing dramatically reduced development of vascular bundles and interfascicular fibers, and enlargement of cortical cells. (C) Longitudinal section of a control stem showing long interfascicular fibers next to the endodermis and small cortical cells. (D) Longitudinal section of a stem of miR165 overexpressors showing interfascicular fibers located several cell layers away from the endodermis and radially swollen cortical cells. Arrows point to parenchymatous cells next to the endodermis in the interfascicular regions. Co, cortex; en, endodermis; if, interfascicular fiber; vb, vascular bundle. Bars = 104 μm in (A) and (B), and 163 μm in (C) and (D).

Downloaded from https://academic.oup.com/pcp/article/48/3/391/2329589 by guest on 21 August 2022

Table 1 Overexpression of miR165 affects the expression of a number of genes involved in auxin biosynthesis and signaling, and vascular development

AGI No.	Annotation	Expression level		Change	Fold	*P*-value
		Control	miR165-OV			
Auxin biosynthesis						
At3g44300	Nitrilase 2 (NIT2)	2,857.9	4677.4	I	1.6	0.020
At3g44320	Nitrilase 3 (NIT3)	91.4	246.1	I	2.7	0.009
Auxin signaling						
At2g33860	ARF3	161.7	313.1	I	1.9	0.050
At5g60450	ARF4	80.2	347.5	I	4.3	0.002
At1g56010	NAC1	82.3	278.1	I	3.4	0.001
At4g08150	KNAT1	123.8	276.1	I	2.2	0.009
At3g23050	IAA7/AXR2	1,448.2	830.8	D	1.7	0.000
At2g22670	IAA8	2,031.0	1,357.8	D	1.5	0.008
At1g04250	IAA17/AXR3	679.3	382.3	D	1.8	0.020
At4g32280	IAA29	183.4	64.7	D	2.8	0.007
At5g19530	Spermine synthase/ACL5	223.6	68.9	D	3.2	0.003
Meristem development						
At5g43810	PNH/ZLL	254.6	154.6	D	1.6	0.004
Vascular development						
At5g64080	Xylogen/AtXYP1	237.6	146.7	D	1.6	0.023
At2g13820	Xylogen/AtXYP2	220.3	64.4	D	3.4	0.015
At5g44030	CESA4/IRX5	153.4	60.1	D	2.6	0.022
At5g17420	CESA7/IRX3	80.7	42.7	D	1.9	0.019
At4g18780	CESA8/IRX1	113.9	43.3	D	2.7	0.045
At4g35350	Cysteine protease/XCP1	138.1	37.1	D	3.8	0.016
At1g20850	Cysteine protease/XCP2	515.9	129.2	D	4.0	0.000

The expression levels listed are the average of hybridization signals from two biological replicates. 'I' represents an increase and 'D' a decrease in gene expression level in miR165 overexpressors (miR165-OV) compared with the control.

inhibits xylem differentiation in stems, which is consistent with the observed defects in the vein development in cotyledons and leaves.

The development of interfascicular fibers was also drastically affected in the stems of miR165 overexpressors. Fewer interfascicular fibers were developed between the vascular bundles, and they had much thinner walls (Fig. 6B). Because interfascicular fibers are essential for the normal stem strength, it is likely that the reduced number and wall thickness of fiber cells contribute to the reduced stem strength of miR165 overexpressors. It was noted that some interfascicular fibers were positioned several cell layers away from the endodermis instead of next to it as seen in the control (Fig. 6C, D), a phenotype reminiscent of the *ifl1* mutant (Zhong and Ye 1999). Another prominent phenotype was a radial enlargement of cortical cells (Fig. 6B, D), which also resembles the *ifl1* mutant (Zhong *et al*. 2001).

Global gene expression analysis in miR165 overexpressors

To investigate what genes are affected by miR165 overexpression, we analyzed the global gene expression in miR165 overexpressors using the Affimetrix *Arabidopsis* oligo microarray. It was found that miR165 overexpression caused a complex up- or down-regulation of many genes (see Supplementary Table 1). Consistent with the defective vascular phenotype, several genes involved in vascular development were down-regulated (Table 1). Although miR165 overexpression severely affected SAM formation, the expression of genes essential for apical meristem formation (Williams and Fletcher 2005), such as *STM*, *WUS* and *AGO1*, was not altered (Supplementary Table 1). The expression of the *PNH/ZLL* gene was slightly reduced (Table 1). Detailed analysis of the microarray data showed that the expression levels of several genes involved in auxin synthesis and signaling were significantly altered (Table 1). While the *ARF3*, *ARF4* (Liscum and Reed 2002) and *NAC1* (Xie *et al*. 2000) genes were up-regulated, several *IAA* genes (Liscum and Reed 2002) and the *ACL5* gene (Clay and Nelson 2005) were down-regulated. The up- or down-regulation of the expression of these genes was further confirmed by quantitative real-time PCR analysis (Fig. 7A, B). It is likely that the alteration in the expression of these genes partly contributes to the pleiotropic

Downloaded from https://academic.oup.com/pcp/article/48/3/391/2329589 by guest on 21 August 2022

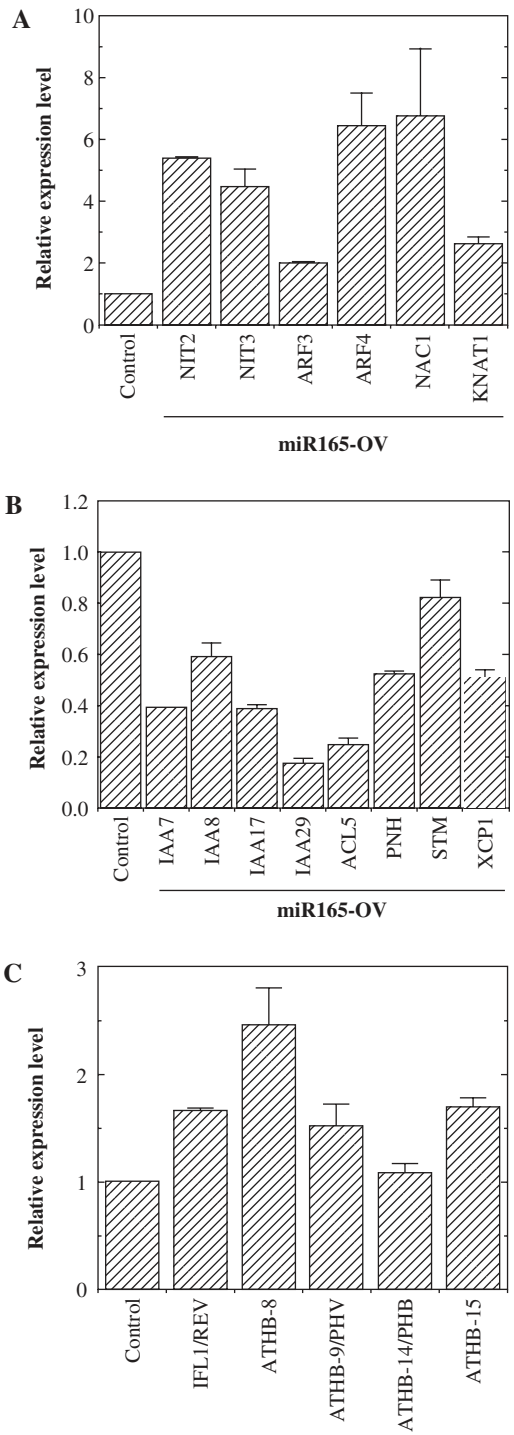

Fig. 7 Quantitative real-time PCR analysis of the expression levels of several representative genes affected by miR165 overexpression and of *HD-ZIP III* genes after auxin treatment. The expression level of each gene in the control seedlings is set to 1. The error bars represent the standard error of triplicate samples. (A) Genes induced by miR165 overexpression. (B) Genes down-regulated by miR165 overexpression. (C) Effects of auxin treatment on the expression of *HD-ZIP III* genes. *Arabidopsis* seedlings were incubated with auxin for 2 h before used for gene expression analysis.

phenotypes caused by miR165 overexpression. These results indicate a link between miR165 overexpression and auxin synthesis and signaling. We further investigated whether auxin treatment causes any effects on the expression of miR165 and *HD-ZIP III* genes. It was found that although the expression of the miR165 gene was not altered (data not shown), several *HD-ZIP III* genes were induced by auxin treatment (Fig. 7C).

Consistent with the observed accumulation of red pigments, genes involved in anthocyanin biosynthesis were found to be highly up-regulated in miR165 overexpressors (Table 2). In addition, PAP1, which is a transcription factor able to activate the whole biosynthetic pathway of anthocyanin when overexpressed (Tohge *et al.* 2005), was also strongly up-regulated (Table 2). It is possible that activation of the anthocyanin biosynthetic pathway in the cotyledons of miR165 overexpressors is a stress response due to the abnormal vascular development. Alternatively, overaccumulation of miR165 could lead to an indirect interference with the expression of non-target genes involved in anthocyanin biosynthesis.

Discussion

HD-ZIP III genes are considered to be targets of miR165/166 based on sequence prediction, biochemical studies and genetic analysis of dominant mutations of *HD-ZIP III* genes. Overexpression of miR166 by activation tagging has been shown to decrease the mRNA levels of *ATHB-9*/*PHV*, *ATHB-14*/*PHB* and *ATHB-15*, and concomitantly cause a phenotype reminiscent of the *phv phb cna* triple mutant (Kim *et al.* 2005, Williams *et al.* 2005). However, it did not mimic the phenotypes exhibited by *rev*/*ifl1* and *rev phb phv* (Prigge *et al.* 2005). In this report, we demonstrate that overexpression of miR165 causes a drastic reduction in the mRNA levels of all five *HD-ZIP III* genes and concomitantly recapitulates the loss-of-function phenotypes of *rev*/*ifl1* and *rev phb phv*, including loss of SAM, altered organ polarity, defective vascular development and impaired interfascicular fiber differentiation. These results suggest that miR165 plays important roles in concert with miR166 in the regulation of *HD-ZIP III* genes, thus influencing plant growth and development.

Our results have shown that overexpression of miR165 leads to a high level accumulation of mature miR165 and a concomitant down-regulation of expression of all five *HD-ZIP III* genes. In contrast, overexpression of miR166, which was shown to result in a high level accumulation of its transcript in embryo, mainly down-regulates the expression of *ATHB-15*, *ATHB-9*/*PHV* and *ATHB-14*/*PHB* (Kim *et al.* 2005, Williams *et al.* 2005), indicating that miR165 and miR166 have differential effects on the regulation of their target genes. This differential regulation

Downloaded from https://academic.oup.com/pcp/article/48/3/391/2329589 by guest on 21 August 2022

Table 2 MiR165 overexpression causes an induction in the expression of genes involved in anthocyanin biosynthesis

AGI No.	Annotation	Expression level		Fold	*P*-value
		Control	miR165-OV		
At3g53260	Phenylalanine ammonia lyase/PAL2	692.1	1,269.8	1.8	0.009
At5g04230	Phenylalanine ammonia lyase/PAL3	140.0	265.9	1.9	0.013
At2g30490	Cinnamate-4-hydroxylase/ C4H	532.4	1015.2	1.9	0.002
At3g21240	4-Coumarate:CoA ligase/ At4CL2	172.2	358.6	2.1	0.024
At5g13930	Chalcone synthase/TT4	211.8	4,582.8	21.6	0.000
At3g55120	Chalcone isomerase/TT5	142.3	411.9	2.9	0.027
At5g05270	Putative chalcone-flavanone isomerase	70.8	407.6	6.0	0.030
At3g51240	Flavanone 3-hydroxylase/ TT6	101.8	1,068.1	10.5	0.002
At5g07990	Flavonoid 3′-hydroxylase/ TT75	51.1	183.5	3.6	0.000
At5g42800	Dihydroflavonol 4-reductase/ TT3	35.4	2,913.3	82.5	0.000
At5g17050	UDP-glucose:flavonoid 3-O-glucosyltransferase-like protein/UGT78D2	101.9	627.0	6.2	0.000
At4g14090	Glucosyltransferase-like protein/UGT75C1	3.0	1,080.5	360.3	0.000
At5g54060	Flavonol 3-O-glucosyltransferase-like/UGT79B1	41.2	1,285.1	31.7	0.003
At3g21560	UDP-glucose:indole-3-acetate β-D-glucosyltransferase/UGT84A2	151.7	321.4	2.1	0.003
At1g30530	UDP-glucose:flavonoid3-O-glucosyltransferase, putative/ FGT	100.7	254.1	2.5	0.008
At2g36790	Putative glucosyl transferase/ FGT	32.8	81.3	2.5	0.031
At3g29590	Anthocyanin 5-aromatic acyltransferase	20.7	309.5	15.5	0.012
At4g22870	Anthocyanidin synthase-like protein	13.6	1,920.0	156.5	0.008
At5g17050	Anthocyanin glycosyltransferase	101.9	627.0	6.2	0.000
At4g14090	Anthocyanin glycosyltransferase	3.0	1,080.5	360.3	0.000
At5g54060	Anthocyanin glycosyltransferase	41.2	1,285.1	31.7	0.003
At3g21560	Anthocyanin glycosyltransferase	151.7	321.4	2.1	0.003
At3g29590	Anthocyanin acyltransferase	20.7	309.5	15.5	0.012
At5g17220	Glutathione S-transferase-like protein/TT19	10.5	1,463.8	157.2	0.009

(continued)

Downloaded from https://academic.oup.com/pcp/article/48/3/391/2329589 by guest on 21 August 2022

Table 2 Continued

AGI No.	Annotation	Expression level		Fold	*P*-value
		Control	miR165-OV		
At1g02930	Glutathione S-transferase/ AtGST6	2,620.1	5,536.5	2.1	0.027
At1g02940	Glutathione S-transferase/ AtGST5	14.2	61.5	4.3	0.000
At1g34580	Putative monosaccharide transporter	61.4	189.4	3.1	0.008
At4g04750	Putative sugar transporter	108.0	234.8	2.2	0.003
At1g56650	Transcription factor/PAP1	26.4	373.8	14.1	0.001

could be due to different effectiveness of miR165 and miR166 on the cleavage of their target genes. Alternatively, the expression level and/or location of miR166 resulting from activation tagging may be different from that of miR165 driven by the CaMV 35S promoter, which could account for the differential effects on the regulation of their target genes. After submission of our manuscript, Jung and Park (2007) reported that both miR165 and miR166 could cleave *REV* mRNA although miR166 does so with a lower efficiency, and ectopic overexpression of miR166 causes a significant reduction only in the expression of *ATHB-9*/*PHV*, *ATHB-14*/*PHB* and *ATHB-15* genes. These results support the possibility that miR165 and miR166 have differential effectiveness for the cleavage of *HD-ZIP III* transcripts. In addition, it was shown that the promoters of three miR165/166 genes direct the expression of the β-glucuronidase (GUS) reporter gene in different tissues, indicating that these miR165/166 genes might regulate their target genes in a tissue-specific manner (Jung and Park 2007).

The differential effects on the regulation of their target genes by overexpression of miR165 and miR166 are also reflected in the resulting plant phenotypes. Overexpression of miR166 results in an enlargement of the SAM (Kim *et al*. 2005, Williams *et al*. 2005), which is reminiscent of the *phv phb cna* triple mutant (Prigge *et al*. 2005). In contrast, overexpression of miR165 causes a loss of SAM and formation of pin-like cotyledons or two narrow cotyledons with a pin or leaf-like structure at the apical region. The pin-like cotyledon phenotype is similar to that exhibited by the *rev phb phv* or *rev phb cna* triple mutant (Prigge *et al*. 2005). This suggests that miR165 and miR166 might affect SAM formation in a different way. It further indicates that a tight regulation of *HD-ZIP III* target genes by miR165 and miR166 is essential for normal meristem development. Recently, it has been shown that ectopic overexpression of miR166 also leads to formation of narrow leaves, but no pin-like cotyledons in the transgenic seedlings were reported (Jung and Park 2007). The lack of formation of pin-like cotyledons could be due to the fact that ectopic overexpression of miR166 only results in a significant reduction in the expression of *ATHB-9*/*PHV*, *ATHB-14*/*PHB* and *ATHB-15* genes (Jung and Park 2007).

The phenotype of two narrow cotyledons without a SAM or with a pin-like structure in miR165 overexpressors is similar to that seen in the mutants with mutations in the *AGO1*-like genes, *AGO1* and *PNH*/*ZLL*. AGO1-like proteins are part of the RNAi silencing complex and they are involved in miRNA binding and cleavage of target mRNAs (Kidner and Martienssen 2005a). The exact mechanisms by which AGO1 and PNH/ZLL regulate meristem function are not known. It has been proposed that AGO1 regulates meristem function via *HD-ZIP III* genes (Kidner and Martienssen 2005b). The *ago1* mutation has been shown to cause mislocalization of miR165 in the meristem, which might result in abnormal cleavage of *HD-ZIP III* transcripts, thus leading to SAM defects (Kidner and Martienssen 2004). Our finding that overexpression of miR165 leads to a phenotype resembling that of the *ago1* mutant provides further evidence that the normal level and location of miR165 are important for meristem function.

In addition to defective SAM, miR165 overexpression causes a severe defect in the polarity of cotyledons, leaves and carpels. The most severe phenotype is formation of radialized cotyledons, which resembles that of the *rev phb phv* triple mutant (Prigge *et al*. 2005). Because the *IFL1*/*REV*, *ATHB-9*/*PHV* and *ATHB-14*/*PHB* genes are expressed on the adaxial side of leaf primordia and thought to determine the adaxial identity (McConnell *et al*. 2001, Otsuga *et al*. 2001), overexpression of miR165 most probably causes abnormal cleavage of *HD-ZIP III* transcripts, thus leading to abaxialization of organs. This is consistent with the fact that the levels of *HD-ZIP III* transcripts are dramatically reduced in miR165 overexpressors. The importance of proper regulation of *HD-ZIP III*

Downloaded from https://academic.oup.com/pcp/article/48/3/391/2329589 by guest on 21 August 2022

genes by miR165 has also been demonstrated by the gain-of-function mutations of *HD-ZIP III* genes. Mutations in the miR165 target sequences of *IFL1*/*REV*, *ATHB-9*/*PHV* and *ATHB-14*/*PHB* cause a resistance to cleavage by miRNA and a drastic alteration in organ polarity (McConnell *et al*. 2001, Emery *et al*. 2003, Zhong and Ye 2004). It should be noted that although organ polarity and the expression of *HD-ZIP III* genes are drastically affected by miR165 overexpression, the expression level of other known polarity genes, including *YABBY*, *KANADI* and *AS* (Bowman *et al*., 2002), is not altered (Supplementary Table 1).

Many of the observed phenotypes in the miR165 overexpressors, such as the altered organ polarity and aberrant development of vascular tissues and fibers, could be due to an alteration in positional information. Auxin is known to be an important positional signal involved in several processes, including vascular differentiation and patterning (Fukuda 2004), and embryo and organ pattern formation (Benková *et al*. 2003, Friml *et al*. 2003). The possibility that auxin might be involved in HD-ZIP III-regulated processes is supported by the finding that the *ifl1* mutation causes a drastic reduction in polar auxin flow along the inflorescence stems. Many of the *ifl1* phenotypes, such as defects in the differentiation of interfascicular fibers and secondary xylem, formation of pin-like inflorescence and a reduction in the production of lateral branches, could be phenocopied by treatment of wild-type *Arabidopsis* with a polar auxin transport inhibitor (Zhong and Ye 2001). The finding that miR165 overexpression results in a complex change in the expression of genes involved in auxin signaling is in agreement with a possible role for auxin in mediation of miR165-regulated processes. Understanding how HD-ZIP III proteins regulate downstream genes will be necessary for further understanding of the molecular mechanisms by which miR165 and HD-ZIP III affect different cellular and biochemical pathways, thus influencing plant growth and development.

Materials and Methods

Generation of miR165-overexpressing plants

Genomic sequences surrounding miR165a on chromosome 1 were PCR-amplified from genomic DNA isolated from wild-type *Arabidopsis thaliana* ecotype Columbia. The amplified DNA was ligated downstream of the CaMV 35S promoter in the binary vector pBI121 (Clontech, Palo Alto, CA, USA) and confirmed by sequencing. The constructs were introduced into wild-type *Arabidopsis* plants (ecotype Columbia) by the *Agrobacterium tumefaciens*-mediated transformation procedure (Bechtold and Bouchez 1994). Transgenic plants were selected on kanamycin, and the first generations were used for gene expression analysis and phenotypic characterization.

Expression analysis

For examination of the steady-state level of mRNAs of genes of interest in the control and miR165 overexpressors, RT–PCR analysis was performed. Total RNA was isolated from 1-week-old seedlings using a Qiagen RNA isolation kit (Qiagen, Valencia, CA, USA). The purified RNA was first treated with DNase I to remove any potential genomic DNA contamination and then used for first strand cDNA synthesis and PCR amplification with gene-specific primers. The primers used for amplification of *HD-ZIP III* mRNAs are located on either side of the miR165 target sequence, so that only the mRNAs not cleaved at the miR165 target site could be used as templates for amplification. The PCRs were performed for various cycles to determine the logarithmic phase of amplifications for all samples. The RT–PCR experiments were repeated three times, and identical results were obtained. The expression of a ubiquitin gene was used as an internal control to determine the efficiency of RT–PCR among different samples.

Quantitative real-time PCR analysis was performed using the QuantiTect SYBR Green PCR kit (Qiagen). The reactions were carried out in the Smart Cycler (Cepheid, Sunnyvale, CA, USA). The relative mRNA levels were calculated by normalizing the PCR threshold cycle number of each gene with that of the EF1α reference gene. The expression level of each gene in the wild-type control was set to 1. The data were the averages of triplicate samples.

RNA gel blot analysis

Total RNA was isolated from 1-week-old seedlings using the TRIzol reagent (Invitrogen, Carlsbad, CA, USA). A 30 μg aliquot of total RNA was separated on a 5% agarose gel and then transferred onto a nylon membrane by capillary (Sambrook *et al*. 1989). miRNA165 was detected using a digoxigenin (DIG)-labeled RNA probe following the protocol described by Ramkissoon *et al*. (2005). Briefly, membranes were pre-hybridized at 42°C using the ULTRAhyb-Oligo buffer (Ambion, Austin, TX, USA), and then hybridized with the 3′-DIG-labeled antisense miR165 RNA probe (150 ng ml^{-1}) (Sigma-Proligo, St Louis, MO, USA) overnight at room temperature. Following hybridization, membranes were washed three times with a low stringency buffer (2× SSC and 0.1% SDS). Hybridized miR165 was detected with the DIG chemiluminiscent detection kit (Roche, Penzberg, Germany) following the manufacturer's protocol.

Auxin treatment

Two-week-old *Arabidopsis* seedlings grown on Murashige and Skoog medium were used for auxin treatment as described (Zhong and Ye 2003). The seedlings were immersed in Murashige and Skoog medium (control), or Murashige and Skoog medium with 50 μM naphthylacetic acid, for 2 h. After treatment, the seedlings were harvested for RNA isolation and subsequent expression analysis.

Microscopy

Plant tissues were fixed in 2% (v/v) glutaraldehyde in phosphate buffer (50 mM, pH 7.2), post-fixed in 1% (v/v) OsO_4 and embedded in Araldite resin (Electron Microscopy Sciences, Fort Washington, PA, USA). Sections 1 μm thick were cut and stained with toluidine blue. For imaging of leaf epidermis, leaves were cryo-prepared, coated with gold and viewed with a LEO982 FE scanning electron microscope (LEO; Thornwood, NY, USA). For visualization of veins, cotyledons and leaves were treated sequentially in 95% (v/v) ethanol, 7% (w/v) NaOH and 250%

Downloaded from https://academic.oup.com/pcp/article/48/3/391/2329589 by guest on 21 August 2022

(w/v) chloral hydrate, and observed with a dissection microscope with dark-field illumination.

Microarray analysis

Total RNA was isolated from 1-week-old seedlings using a Qiagen RNA isolation kit. RNA from two independent isolations was used for microarray analysis using ATH1 GeneChip™ (Affymetrix, Santa Clara, CA, USA) according to Kubo *et al*. (2005). A 10 μg aliquot of RNA was reverse transcribed using the SuperScript Choice System for cDNA synthesis (Invitrogen) and employing the protocol recommended by Affymetrix. A 1 μg aliquot of cDNA was used for in vitro transcription with the Enzo BioArray High Yield RNA transcript labeling kit (Enzo Diagnostics, Farmingdale, NY, USA). The cRNA thus synthesized was cleaned using RNAeasy clean-up columns (Qiagen) and then fragmented by heating in 40 mM Tris-acetate (pH 8.1), 100 mM KOAc, 30 mM MgOAc. The Affymetrix eukaryotic hybridization controls were added to the samples prior to hybridization according to the manufacturer's instructions. Affymetrix Arabidopsis ATH1 GeneChip arrays were hybridized with 10 μg of fragmented cRNA. Washing and staining were performed in a Fluidics Station 400 (Affymetrix), and the arrays were scanned in an Affymetrix GeneChip scanner. Data analysis was done using the Affymetrix Microarray Analysis Suite software (version 5.0). Two independent experiments were performed for each experimental condition, and the output of the data analysis from the Affymetrix Microarray Suite software for each independent experiment was subjected to further analysis using Microsoft Excel (Solfanelli *et al*. 2006). Differences in transcript abundance, expressed as signal log ratio, were calculated using the Microarray Suite software software change algorithm. The signal log ratio was assumed to be correct only if the corresponding change call indicated a significant change (I, increase; D, decrease). Expression data were filtered to select only genes showing a coinciding change call and a P-value ≤ 0.05 in the two biological samples. Fold changes were calculated based on the log transformed data of two biological replicates.

Supplementary material

Supplementary material mentioned in the article is available to online subscribers at the journal website www.pcp.oxfordjournals.org.

Acknowledgments

We thank Dr. R.R. Walcott for his help on real-time PCR analysis, E.A. Richardson and J. Wu for their help on microscopy, and the editor and reviewers for their constructive comments and suggestions. This work was supported by grants from the U.S. Department of Energy-Bioscience Division (Z.H.Y.) and the Japan Society for the Promotion of Science (T.D).

References

Bechtold, N. and Bouchez, D. (1994) *In* planta *Agrobacterium*-mediated transformation of adult *Arabidopsis thaliana* plants by vacuum infiltration. *In* Gene Transfer to Plants. Edited by Potrykus, I. and Spangenberg, G. pp. 19–23. Springer-Verlag, Berlin.

Benková, E., Michniewicz, M., Sauer, M., Teichmann, T., Seifertová, D., Jürgens, G. and Friml, J. (2003) Local, efflux-dependent auxin gradients as a common module for plant organ formation. *Cell*. 115: 591–602.

Bowman, J.L., Eshed, Y. and Baum, S.F. (2002) Establishment of polarity in angiosperm lateral organs. *Trends Genet*. 18: 134–141.

Chen, X. (2005) MicroRNA biogenesis and function in plants. *FEBS Lett*. 579: 5923–5931.

Dugas, D.V. and Bartel, B. (2004) MicroRNA regulation of gene expression in plants. *Curr. Opin. Plant Biol*. 7: 512–520.

Clay, N.K. and Nelson, T. (2005) *Arabidopsis* thickvein mutation affects vein thickness and organ vascularization, and resides in a provascular cell-specific spermine synthase involved in vein definition and in polar auxin transport. *Plant Physiol*. 138: 767–77.

Emery, J.F., Floyd, S.K., Alvarez, J., Eshed, Y., Hawker, N.P., Izhaki, A., Baum, S.F. and Bowman, J.L. (2003) Radial patterning of *Arabidopsis* shoots by class III HD-ZIP and KANADI genes. *Curr. Biol*. 13: 1768–1774.

Friml, J., Vieten, A., Sauer, M., Weijers, D., Schwarz, H., Hamann, T., Offringa, R. and Jurgens, G. (2003) Efflux-dependent auxin gradients establish the apical–basal axis of *Arabidopsis*. *Nature*. 426: 147–153.

Fukuda, H. (2004) Signals that control plant vascular cell differentiation. *Nature Rev. Mol. Cell Biol*. 5: 379–391.

Green, K.A., Prigge, M.J., Katzman, R.B. and Clark, S.E. (2005) *CORONA*, a member of the class III homeodomain leucine zipper gene family in *Arabidopsis*, regulates stem cell specification and organogenesis. *Plant Cell*. 17: 691–704.

Jover-Gil, S., Candela, H. and Ponce, M.-R. (2005) Plant microRNAs and development. *Int. J. Dev. Biol*. 49: 733–744.

Juarez, M.T., Kui, J.S., Thomas, J., Heller, B.A. and Timmermans, M.C. (2004) MicroRNA-mediated repression of *rolled leaf1* specifies maize leaf polarity. *Nature*. 428: 84–88.

Jung, J.-H. and Park, C.-M. (2007) *MIR166/165* genes exhibit dynamic expression patterns in regulating shoot apical meristem and floral development in *Arabidopsis*. *Planta* in press.

Kidner, C.A. and Martienssen, R.A. (2004) Spatially restricted microRNA directs leaf polarity through *ARGONAUTE1*. *Nature*. 428: 81–84.

Kidner, C.A. and Martienssen, R.A. (2005a) The developmental role of microRNA in plants. *Curr. Opin. Plant Biol*. 8: 38–44.

Kidner, C.A. and Martienssen, R.A. (2005b) The role of ARGONAUTE1 (AGO1) in meristem formation and identity. *Dev. Biol*. 280: 504–517.

Kim, J., Jung, J.-H., Reyes, J.L., Kim, Y.-S., Kim, S.-Y., et al. (2005) MicroRNA-directed cleavage of *ATHB15* mRNA regulates vascular development in Arabidopsis inflorescence stems. *Plant J*. 42: 84–94.

Kubo, M., Udagawa, M., Nishikubo, N., Horiguchi, G., Yamaguchi, M., Ito, J., Mimura, T., Fukuda, H. and Demura, T. (2005) Transcription switches for protoxylem and metaxylem vessel formation. *Genes Dev*. 19: 1855–1860.

Kurihara, Y. and Watanabe, Y. (2004) *Arabidopsis* micro-RNA biogenesis through Dicer-like 1 protein functions. *Proc. Natl Acad. Sci. USA*. 101: 12753–12758.

Li, H., Xu, L., Wang, H., Yuan, Z., Cao, X., Yang, Z., Zhang, D., Xu, Y. and Huang, H. (2005) The putative RNA-dependent RNA polymerase RDR6 acts synergistically with ASYMMETRIC LEAVES1 and 2 to repress BREVIPEDICELLUS and MicroRNA165/166 in *Arabidopsis* leaf development. *Plant Cell*. 17: 2157–2171.

Liscum, E. and Reed, J.W. (2002) Genetics of Aux/IAA and ARF action in plant growth and development. *Plant Mol. Biol*. 49: 387–400.

McConnell, J.R. and Barton, M.K. (1998) Leaf polarity and meristem formation in *Arabidopsis*. *Development*. 125: 2935–2942.

McConnell, J.R., Emery, J., Eshed, Y., Bao, N., Bowman, J. and Barton, M.K. (2001) Role of *PHABULOSA* and *PHAVOLUTA* in determining radial patterning in shoots. *Nature*. 411: 709–713.

McHale, N.A. and Koning, R.E. (2004) MicroRNA-directed cleavage of *Nicotiana sylvestris PHAVOLUTA* mRNA regulates the vascular cambium and structure of apical meristems. *Plant Cell*. 16: 1730–1740.

Ochando, I., Jover-Gil, S., Ripoll, J.J., Candela, H., Vera, A., Ponce, M.R., Martinez-Laborda, A. and Micol, J.L. (2006) Mutations in the microRNA complementarity site of the *INCURVATA4* gene perturb meristem function and adaxialize lateral organs in *Arabidopsis*. *Plant Physiol*. 141: 607–619.

Ohashi-Ito, K., Demura, T. and Fukuda, H. (2002) Promotion of transcript accumulation of novel *Zinnia* immature xylem-specific HD-Zip III homeobox genes by brassinosteroids. *Plant Cell Physiol*. 43: 1146–1153.

Downloaded from https://academic.oup.com/pcp/article/48/3/391/2329589 by guest on 21 August 2022

Ohashi-Ito, K. and Fukuda, H. (2003) HD-Zip III homeobox genes that include a novel member, *ZeHB-13* (*Zinnia*)/*ATHB-15* (*Arabidopsis*), are involved in procambium and xylem cell differentiation. *Plant Cell Physiol*. 44: 1350–1358.

Ohashi-Ito, K., Kubo, M., Demura, T. and Fukuda, H. (2005) Class III homeodomain leucine-zipper proteins regulate xylem cell differentiation. *Plant Cell Phsyiol*. 46: 1646–1656.

Otsuga, D., DeGuzman, B., Prigge, M.J., Drews, G.N. and Clark, S.E. (2001) *REVOLUTA* regulates meristem initiation at lateral positions. *Plant J*. 25: 223–236.

Prigge, M.J., Otsuga, D., Alonso, J.M., Ecker, J.R., Drews, G.N. and Clark, S.E. (2005) Class III homeodomain-leucine zipper gene family members have overlapping, antagonistic, and distinct roles in *Arabidopsis* development. *Plant Cell*. 17: 61–76.

Ramkissoon, S.H., Mainwaring, L.A., Sloand, E.M., Young, N.S. and Kajigaya, S. (2006) Nonisotopic detection of microRNA using digoxigenin labeled RNA probes. *Mol. Cell Probes*. 20: 1–4.

Reinhart, B.J., Weinstein, E.G., Rhoades, W.W., Bartel, B. and Bartel, D.P. (2002) MicroRNA in plants. *Genes Dev*. 16: 1616–1626.

Rhoades, M.W., Reinhart, B.J., Lim, L.P., Burge, C.B., Bartel, B. and Bartel, D.P. (2002) Prediction of plant microRNA targets. *Cell*. 110: 513–520.

Sambrook, J., Fritsch, E.F. and Maniatis, T. (1989) Molecular Cloning: A Laboratory Manual. Cold Spring Harbor Laboratory Press, Cold Spring Harbor, NY.

Solfanelli, C., Poggi, A., Loreti, E., Alpi, A. and Perata, P. (2006) Sucrose-specific induction of the anthocyanin biosynthetic pathway in *Arabidopsis*. *Plant Physiol*. 140: 637–646.

Tang, G., Reinhart, B.J., Bartel, D.P. and Zamore, P.D. (2003) A biochemical framework for RNA silencing in plants. *Genes Dev*. 17: 49–63.

Tohge, T., Nishiyama, Y., Hirai, M.Y., Yano, M., Nakajima, J., et al. (2005) Functional genomics by integrated analysis of metabolome and transcriptome of *Arabidopsis* plants over-expressing an MYB transcription factor. *Plant J*. 42: 218–35.

Williams, L. and Fletcher, J.C. (2005) Stem cell regulation in the *Arabidopsis* shoot apical meristem. *Curr. Opin. Plant Biol*. 8: 582–586.

Williams, L., Grigg, S.P., Xie, M., Christensen, S. and Fletcher, J.C. (2005) Regulation of *Arabidopsis* shoot apical meristem and lateral organ formation by microRNA *miR166g* and its *AtHD-ZIP* target genes. *Development*. 132: 3657–3668.

Xie, Q., Frugis, G., Colgan, D. and Chua, N.-H. (2000) *Arabidopsis* NAC1 transduces auxin signal downstream of TIR1 to promote lateral root development. *Genes Dev*. 14: 3024–3036.

Zhang, B., Pan, X., Cobb, G.P. and Anderson, T.A. (2006) Plant microRNA: a small regulatory molecule with big impact. *Dev. Biol*. 289: 3–16.

Zhong, R., Burk, D.H. and Ye, Z.-H. (2001) Fibers. A model for studying cell differentiation, cell elongation, and cell wall biosynthesis. *Plant Physiol*. 126: 477–479.

Zhong, R., Taylor, J.J. and Ye, Z.-H. (1999) Transformation of the collateral vascular bundles into amphivasal vascular bundles in an *Arabidopsis* mutant. *Plant Physiol*. 120: 53–64.

Zhong, R. and Ye, Z.-H. (1999) *IFL1*, a gene regulating interfascicular fiber differentiation in *Arabidopsis*, encodes a homeodomain-leucine zipper protein. *Plant Cell*. 11: 2139–2152.

Zhong, R. and Ye, Z.-H. (2001) Alteration of auxin polar transport in the *Arabidopsis ifl1* mutants. *Plant Physiol*. 126: 549–563.

Zhong, R. and Ye, Z.-H. (2003) The SAC domain-containing protein gene family in *Arabidopsis*. *Plant Physiol*. 132: 544–555.

Zhong, R. and Ye, Z.-H. (2004) *amphivasal vascular bundle 1*, a gain-of-function mutation of the *IFL1*/*REV* gene, is associated with alterations in the polarity of leaves, stems and carpels. *Plant Cell Physiol*. 45: 369–385.

(Received December 20, 2006; Accepted January 11, 2007)

Downloaded from https://academic.oup.com/pcp/article/48/3/391/2329589 by guest on 21 August 2022